CONVECTIVE MOTION IN A CLOSED VERTICAL CAVITY WITH PERMEABLE LATERAL WALLS

V. A. Mochalov and M. K. Vermishev

UDC 536.25

Velocity and temperature distributions are obtained for $0 \leq \mathrm{Ra} \leq 2 \cdot 10^5$ and various rates of transverse flow in a vertical cavity with permeable lateral walls.

The existing analytical studies of thermal convection in a closed vertical cavity have been carried out for the case of impermeable lateral walls [1-7].

We consider plane convective motion of a viscous incompressible fluid in a closed vertical cavity with permeable lateral walls, an aspect ratio $l = H/L$ and a constant lateral-wall temperature (Fig. 1).

We use the temperature at the vertical wall at x = 0 as a zero point and the temperature is θ_w at the wall at x = L. The temperature varies linearly along the lower base at y = 0 and along the upper base at y = H. Gravity is directed vertically downwards.

The vertical surfaces of the cavity are assumed to be permeable. Uniform injection of the fluid at a constant rate along the y axis occurs through the surface at x = 0 and uniform suction at the same rate takes place through the surface at x = L.

The equations of motion for the stream function ψ and the temperature function θ, written in dimensionless form, are

$$\frac{1}{\mathrm{Pr}} \frac{\partial \Delta\psi}{\partial t} = \Delta\Delta\psi - \mathrm{Ra} \frac{\partial \theta}{\partial x} - \frac{1}{\mathrm{Pr}} \left(\frac{\partial \psi}{\partial y} \frac{\partial \Delta\psi}{\partial x} - \frac{\partial \psi}{\partial x} \frac{\partial \Delta\psi}{\partial y} \right), \tag{1}$$

$$\frac{\partial \theta}{\partial t} = \Delta\theta - \left(\frac{\partial \psi}{\partial y} \frac{\partial \theta}{\partial x} - \frac{\partial \psi}{\partial x} \frac{\partial \theta}{\partial y} \right). \tag{2}$$

In Eqs. (1) and (2), the following scale factors are assumed for the variables: distance, cavity width L; time, L^2/a; temperature, θ_w; stream function, a. The dimensionless criteria appearing in the equations are the Rayleigh and Prandtl numbers;

$$\mathrm{Ra} = \frac{g\beta\theta_w L^3}{\nu a}, \quad \mathrm{Pr} = \frac{\nu}{a}.$$

The dimensionless velocity of the fluid is associated with the stream function through the relations

$$V_x = \frac{\partial \psi}{\partial y}, \quad V_y = -\frac{\partial \psi}{\partial x},$$

and the Poisson equation for the vorticity takes the form

$$-\Delta\psi = \varphi. \tag{3}$$

We consider a stationary solution of the equation system (1)-(3), i.e., a solution for which the time derivatives of the functions ψ and θ are zero. To obtain a stationary solution, the limiting method is used, i.e., a limiting solution of the nonstationary system (1)-(3) is sought which is independent of the time t to a given accuracy.

Translated from Inzhenerno-Fizicheskii Zhurnal, Vol. 26, No. 4, pp. 594-601, April, 1974.

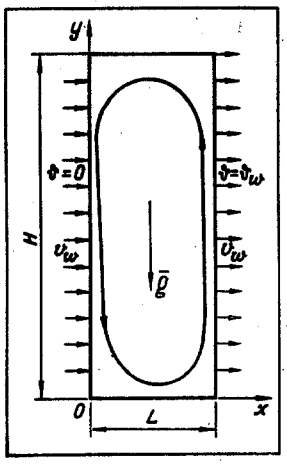

Fig. 1. Coordinate system.

Further, in order to make the calculations with respect to each of Eqs. (1)-(3) identical, the term $\partial\psi/\partial t$ is added to Eq. (3) and this equation is replaced by

$$\frac{\partial\psi}{\partial t} = \varphi + \Delta\psi.$$

It should be noted that introduction of the term $\partial\psi/\partial t$ avoids the need for a separate iterative process for solution of the Poisson equation in each time of the main iterative procedure.

Thus the initial system (1)-(2) is replaced by

$$\frac{1}{\mathrm{Pr}}\frac{\partial\varphi}{\partial t} = \Delta\varphi + \mathrm{Ra}\frac{\partial\theta}{\partial x} - \frac{1}{\mathrm{Pr}}\left(\frac{\partial\psi}{\partial y}\frac{\partial\varphi}{\partial x} - \frac{\partial\psi}{\partial x}\frac{\partial\varphi}{\partial y}\right), \tag{4}$$

$$\frac{\partial\theta}{\partial t} = \Delta\theta - \left(\frac{\partial\psi}{\partial y}\frac{\partial\theta}{\partial x} - \frac{\partial\psi}{\partial x}\frac{\partial\theta}{\partial y}\right), \tag{5}$$

$$\frac{\partial\psi}{\partial t} = \varphi + \Delta\psi \tag{6}$$

with the boundary conditions

$$\begin{aligned}
&\theta = 0, \quad \frac{\partial\psi}{\partial x} = 0, \quad \frac{\partial\psi}{\partial y} = C \quad \text{for} \quad x = 0,\\
&\theta = 1, \quad \frac{\partial\psi}{\partial x} = 0, \quad \frac{\partial\psi}{\partial y} = C \quad \text{for} \quad x = 1,\\
&\theta = x, \quad \frac{\partial\psi}{\partial x} = 0, \quad \frac{\partial\psi}{\partial y} = 0 \quad \text{for} \quad x = 0,\ l.
\end{aligned} \tag{7}$$

In the boundary conditions, the constant C is the Peclet number, which defines the intensity of the transverse flow:

$$\mathrm{Pe} = \frac{v_w L}{a}.$$

The method of finite differences is used to obtain a numerical solution of the system (4)-(6) under the boundary conditions (7).

In the region of integration, we introduce a space–time grid with the mesh points

$$\begin{aligned}
x_i &= ih \quad (i = 0, 1, 2, \ldots, n),\\
y_j &= js \quad (j = 0, 1, 2, \ldots, m),\\
t_k &= k\tau \quad (k = 0, 1, 2, \ldots),
\end{aligned}$$

where h = 1/n is the spacing along the x axis; s = 1/m is the spacing along the y axis; τ is the time step.

We write Eqs. (4)-(6) in finite-difference form by replacing all differential expressions by finite-difference relations:

$$\varphi_{i,j}^{k+1} = \varphi_{i,j}^{k} + \tau\left\{\frac{\mathrm{Ra}}{2h}(\theta_{i+1,j}^{k} - \theta_{i-1,j}^{k}) + \Delta\varphi_{i,j}^{k}\right.$$

$$\left. - \frac{1}{\mathrm{Pr}\,4hs}\left[(\psi_{i,j+1}^{k} - \psi_{i,j-1}^{k})(\varphi_{i+1,j}^{k} - \varphi_{i-1,j}^{k}) - (\psi_{i+1,j}^{k} - \psi_{i-1,j}^{k})(\varphi_{i,j+1}^{k} - \varphi_{i,j}^{k})\right]\right\}, \tag{8}$$

$$\theta_{i,j}^{k+1} = \theta_{i,j}^{k} + \tau\left\{\Delta\theta_{i,j}^{k} - \frac{1}{4hs}\left[(\psi_{i,j+1}^{k} - \psi_{i,j-1}^{k})(\theta_{i+1,j}^{k} - \theta_{i-1,j}^{k}) - (\psi_{i+1,j}^{k} - \psi_{i-1,j}^{k})(\theta_{i,j+1}^{k} - \theta_{i,j-1}^{k})\right]\right\}, \tag{9}$$

$$\psi_{i,j}^{k+1} = \psi_{i,j}^{k} + \tau(\varphi_{i,j}^{k} + \Delta\varphi_{i,j}^{k}). \tag{10}$$

In Eqs. (8)-(10), the Laplacians $\Delta\varphi_{i,j}^{k}$ and $\Delta\theta_{i,j}^{k}$ are approximated by

$$\Delta f_{i,j}^{k} = \frac{f_{i+1,j} + f_{i-1,j} - 2f_{i,j}}{h^2} + \frac{f_{i,j+1} + f_{i,j-1} - 2f_{i,j}}{s^2}.$$

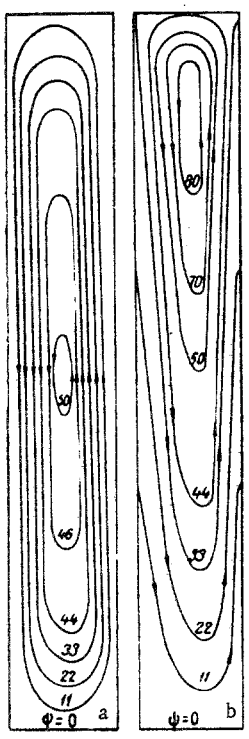

Fig. 2. Streamlines in a cavity for Ra = $6.8 \cdot 10^4$, H/L = 6.6; a) Pe = 0; b) Pe = 2.

In finite-difference form, Eq. (3) becomes

$$\left.\begin{aligned} \varphi_{i,0} &= -\frac{2\psi_{i,1}}{s^2}, \\ \varphi_{i,m} &= -\frac{2\psi_{i,m-1}}{s^2} + \frac{2Cl}{s^2}, \end{aligned}\right\} \quad i = 1, 2, \ldots, n-1,$$

$$\left.\begin{aligned} \varphi_{n,j} &= -\frac{2\psi_{n-1,j}}{h^2} + \frac{2Cjs}{h^2}, \\ \varphi_{0,j} &= -\frac{2\psi_{i,j}}{h^2} - \frac{2Cjs}{h^2}, \end{aligned}\right\} \quad j = 1, 2, \ldots, m-1. \tag{11}$$

The boundary conditions (7) take the form

$$\begin{aligned} &\theta_{0,j} = 0, \quad \theta_{n,j} = 1, \quad \theta_{i,0} = \theta_{i,m} = ih, \\ &\psi_{i,0} = \psi_{i,m} = 0, \quad \varphi_{0,j} = \varphi_{n,j} = Cjs, \\ &i = 0, 1, \ldots, n; \quad j = 0, 1, \ldots, m. \end{aligned} \tag{12}$$

A stationary solution of the system (8)-(10) under the boundary conditions (11)-(12) is realized through the following iterative procedure. Values of ψ and θ are assigned at boundary mesh points on the basis of the conditions (12). We further assume φ, ψ, and θ are zero at all interior mesh points. On the basis of these values, values of the function φ at the boundary mesh points are calculated from Eqs. (11). The resultant system of values for ψ, θ, and φ at all the mesh points (except the vertices of the region) is taken as the zeroth iteration. The iterative step involves the calculation of the quantities ψ^{k+1}, θ^{k+1}, and φ^{k+1} at all the internal mesh points from the values of ψ, θ, and φ by means of Eqs. (8)-(10). Following this, φ^{k+1} at the boundary mesh points is calculated from Eqs. (11). This iterative procedure is repeated until the conditions

$$|\varphi^{k+1} - \varphi^k|_{i,j} < \varepsilon, \quad |\theta^{k+1} - \theta^k|_{i,j} < \varepsilon, \quad |\psi^{k+1} - \psi^k|_{i,j} < \varepsilon,$$

are satisfied in two successive iterations, where ε is the required degree of accuracy of the solution.

The time step was selected on the basis of the convergence conditions for the method. The main calculations were carried out on a 21 × 21 grid with $\tau = 1/4000$ and $\varepsilon = 0.001$. To check the accuracy of the calculations, a number of versions were calculated for 21 × 41 and 21 × 101 meshes to third order accuracy. The iterative procedure continued to be convergent with the first three numbers after the decimal point remaining unchanged but the number of iterations rose to 2000.

The quality of the difference mode was checked by the behavior of the deviation in each iterative step. The computation was carried out until the deviation became less than $\varepsilon = 0.000976$. A stationary solution was realized for versions in which the deviation fell monotonically. For $Ra > 2 \cdot 10^5$, the behavior of the deviation changed markedly and its value began to oscillate. In this case, the values of the functions ψ and θ in the wall regions varied continuously. In all probability, such behavior of the functions ψ and θ was connected with the development of small-scale pulsed motions in the wall region and the production of a stationary solution became impossible in principle.

All the calculations were performed on the Razdan computer.

Stationary solutions were obtained for the following parameter values, which define flow and heat transport: Ra = $5 \cdot 10^2$, 10^3, $5 \cdot 10^3$, $6.8 \cdot 10^4$, 10^5, and $2 \cdot 10^5$; Pe = 0.1, 2, 3, and 5; H/L = 0.5, 1, 2, 4, 6.6, and 10; Pr = 1.

The results presented were obtained for the case of injection into the cold wall and suction from the heated wall. A number of calculations were performed for the opposite transverse flow direction (injection into the heated wall and suction from the cold wall). Calculations for both cases showed that a displacement of the velocity and temperature fields in the cavity from their positions for Pe = 0 in the direction of the wall to which suction was applied occurred under the influence of the transverse flow. Furthermore, injection (suction) through the heated wall had the same effect on flow and heat transfer in the wall region as injection (suction) through the cold wall.

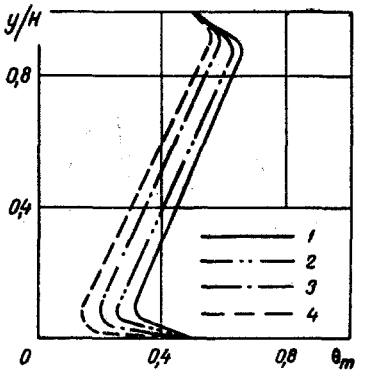

Fig. 3

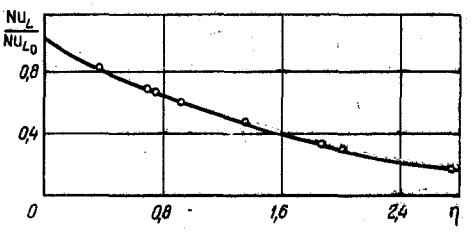

Fig. 4

Fig. 3. Dimensionless temperature in the central vertical section of the cavity: 1) Pe = 0; 2) 1; 3) 2; 4) 3.

Fig. 4. Effect of wall permeability on heat transfer in a cavity. Points are obtained from the present numerical calculations.

From the calculations of the velocity and temperature fields, a systematic shift of the flow and heat-transfer modes was observed depending on the Rayleigh number and the ratio of the sides, and the effect of wall permeability on the flow and heat-transfer structure was also determined.

The results of the calculations for the absence of transverse flow, Pe = 0, is not discussed in detail because this problem was solved previously [4, 6, 7].

With transverse flow present, a nonzero transverse component of the velocity appears at the lateral walls of the cavity. In this case, convective motion in the cavity results not only from gravitational forces but also from transverse flow at constant velocity. Because of very low velocities in the boundary layer during natural convection, the transverse perturbations have a rather strong influence on flow and heat transfer. The effect of transverse flow on the flow structure for $Ra = 6.8 \cdot 10^4$ is shown in Fig. 2b. The streamlines obtained give a representation of the nature of the overall motion arising as the result of the superposition of transverse flow on free convective motion. It is clear from the figure that transverse flow reduces the intensity of circulatory motion and disturbs the symmetry of the flow; in this case, the streamlines are displaced somewhat toward the wall where suction is applied.

Analysis of the flow fields obtained showed that the degree of deformation of free convective motion under the influence of a transverse flow (for fixed velocity of the transverse flow) depends on the Rayleigh number.

For weak convection the velocities are low, which leads to strong displacement of the main flow by the transverse flow. In this case, the slow movement of gas along closed trajectories is preserved only in the upper half of the cavity.

As the Rayleigh number increases, the velocity of free motion rises and the effect of the transverse flow drops. For large Rayleigh numbers and transverse flow, circulatory motion continues to be maintained over the greater portion of the cavity (Fig. 2b).

Analysis of the results of the numerical computation made it possible to establish that with an increase in the intensity of transverse flow, the velocity profile at the cold wall (injection) becomes less complete, the velocity maximum is reduced, and its coordinate is moved away from the wall. At the heated wall (suction), the velocity profile becomes more complete, its maximum is also reduced, and it is displaced toward the wall.

Injection lowers the temperature gradient at the wall, which leads to weakening of heat transfer. Suction has the opposite effect — the gradient at the wall is increased leading to balancing and intensification of heat transfer.

Figure 3 shows the variation of the dimensionless temperature in the central vertical section of the cavity under the influence of transverse flow with $Ra = 6.8 \cdot 10^4$. Depending on direction, the transverse flow reduces or increases the temperature in the central vertical section. The deviation of this temperature from the initial value for Pe = 0 increases as the velocity of the transverse flow increases.

The total thermal flux (per unit length along the y axis) is determined by the distribution of the local values and is

$$Q = -\lambda \int_0^H \left(\frac{\partial T}{\partial x}\right)_w dy. \tag{13}$$

The dimensionless Nusselt number normalized to the width of the cavity is

$$\mathrm{Nu}_L = \frac{QL}{\lambda \theta_w} = \frac{1}{H/L} \int_0^{H/L} \left(\frac{\partial \theta}{\partial x}\right)_w dy = \frac{\lambda_e}{\lambda}. \tag{14}$$

The achievement of thermal balance ($Q_{x=L} = Q_{x=0}$) was checked in the stationary mode with transverse flow absent. The deviation in the total balance was no more than 3% for a 21 × 21 mesh.

With transverse flow present, the equation of thermal balance written in dimensionless form is

$$(\mathrm{Nu}_L)_{x=1} + (\mathrm{Nu}_L)_{x=0} + \mathrm{Pe} = 0. \tag{15}$$

The amount of influence of transverse flow on heat transfer through the cavity in accordance with the results of the analysis of the numerical computation and from a comparison with experiment can be taken into account by the dimensionless permeability parameter $\eta = \mathrm{Pe}\,\lambda/\lambda_e$ which characterizes the ratio between the amount of heat transported by the transverse flow and the amount of heat transferred by the equivalent thermal conductivity.

The variation of heat flow through a cavity associated with the injection process in the Ra and Pe range covered is approximated by

$$\frac{\mathrm{Nu}_L}{\mathrm{Nu}_{L_0}} = \frac{\eta}{\exp \eta - 1}. \tag{16}$$

Curves of the relation (16) are shown in Fig. 4.

The dimensionless temperature in the central vertical section of the cavity including the effect of transverse flow is given by

$$\theta_w = (1 - 0.29\eta)\left(0{,}25 + 0.5\,\frac{y}{H}\right). \tag{17}$$

When $\eta \to 0$, the indeterminacy in Eq. (16) can be removed by use of L'Hopital's rule. After simple transformations, Eq. (16) transforms into the usual formula for the calculation of heat transfer through a vertical layer with impermeable lateral walls.

NOTATION

x	is the longitudinal coordinate;
y	is the transverse coordinate;
V_x, V_y	are the projections of the velocity on the x and y axes;
T	is the temperature;
$\theta = (T-T_1)/(T_2-T_1)$	is the dimensionless temperature of the layer;
ν, λ, a, β, α	are the kinematic viscosity, the thermal conductivity, the thermal diffusivity, the volume expansion, and the heat exchange, respectively;
g	is the acceleration due to gravity;
H, L	are the height and width of the cavity;
λ_e	is the equivalent thermal conductivity;
ψ	is the dimensionless flow function;
t	is the time;
$\mathrm{Ra} = g\beta\theta_w L^3/\nu a$, $\mathrm{Pr} = \nu/a$, $\mathrm{Pe} = v_w L/\nu$	are the Reyleigh, Prandtl, and Peclet numbers;
Q	is the total heat flux per unit length along the y axis;
$\mathrm{Nu}_L = QL/\lambda\theta_w$	is the Nusselt number;
$l = H/L$	is the dimensionless length;
$\eta = \mathrm{Pe}(\lambda/\lambda_e)$	is the dimensionless permeability parameter;
v_w	is the injection (suction) velocity at the side surfaces surfaces of the cavity;
$\theta_w = T_2 - T_1$.	

Subscripts

L denotes mean value;
m denotes value at central vertical section;
0 denotes value on impermeable surface.

LITERATURE CITED

1. G. K. Batchelor, Quarterly of Applied Mathematics, 12, No. 3 (1951).
2. G. Poots, Quarterly J. of Mech. and Applied Math., 11, pt. 3 (1958).
3. A. F. Lietzke, NASA Rep. 1223 (1955).
4. A. F. Emery and N. C. Chu, J. Heat Transfer, 87, 110 (1965).
5. G. de Vahl Davis and C. F. Kettleborough, Mech. and Chem. Engng. Trans. Inst. Engr. Austral., No. 1 (1965).
6. I. O. Wilkes and S. W. Churchill, AIChE Journal, 12, No. 11 (1966).
7. G. Z. Gershuni, E. M. Zhukhovitskii, and E. A. Tarunin, MZhG, No. 5 (1966).
8. M. K. Vermishev and V. A. Mochalov, in: Studies in Structural Physics [in Russian], No. 12 (1) (1969), pp. 76-81.